

Misalignment Studies in Laser Diode to Upside Down Tapered Microlens Tipped Circular Core Photonic Crystal Fiber Excitation

Sumanta Mukhopadhyay*

Department of Physics, St. Paul's Cathedral Mission College, 33/1 Raja Rammohan Roy Sarani, Kolkata, West Bengal, India

Abstract

By employing Gaussian field distributions for both the source and the fiber and also the already derived ABCD matrix for upside down tapered microlens, we investigate theoretically the coupling optics involving a laser diode emitting practically interesting two different wavelengths either $1.3\ \mu\text{m}$ or $1.5\ \mu\text{m}$, and a series of circular core photonic crystal fibers with different air filling ratio and lattice constant via upside down tapered microlens of two specific taper lengths on the tip of such fiber in absence and presence of possible transverse and angular misalignments. It is observed that, for a fit taper length of $70.0\ \mu\text{m}$ of upside down tapered microlens, photonic crystal fiber with air filling ratio of 0.35 and lattice constant of $5.0\ \mu\text{m}$ comes out to be the most suitable one to couple laser diode emitting light of wavelength $\lambda = 1.3\ \mu\text{m}$. The coupling efficiency can reach to 94.63% with simultaneous optimization of taper length and source position of specific lensed fiber. Such analysis which as per our knowledge is the first theoretical investigation, will be extremely important in ongoing investigations for the design of optimum launch optics involving upside down tapered microlens on the tip of photonic crystal fiber. Moreover, the results are extremely useful for assessing deeply the sensitivity of such coupler with reference to above kind of misalignments.

Keywords: ABCD matrix, upside down tapered microlens, circular core photonic crystal fiber, transverse misalignment, angular misalignment

*Author for Correspondence E-mail: sumukherjee_74@yahoo.com

INTRODUCTION

The design and fabrication of integral microlenses on the tip of the single mode fiber (SMF) is of tremendous importance for constructing practical fiber transmission networks employing erbium-doped optical fiber amplifiers as far as efficient coupling between laser diodes (LDs) and SMFs is concerned. These microlenses, whether conical or hemispherical, possess the advantage of being self-centred. Such microlenses may have hyperbolic, hemispherical, parabolic surfaces for modulating the spot size of LD light incident on them and properly match and couple with the fiber spot size [1–13]. However, as it is not precisely possible to form the microlens on the tip of the fiber at the ideally set position as illustrated in Figure 1, the limitations of fabrication of the said type of coupler may lead to relative shift between the microlens output and the fiber input faces resulting in

two possible misalignments, namely, transverse and angular mismatches [14]. Thus, the study of losses incurring due to these two types of misalignments is of immense importance for coupling of LD via microlens on the tip of SMF. Amongst different proposed methods for optimization of coupling efficiency in absence and presence of possible misalignments, the very simple, accurate, elegant and least computable ABCD matrix technique has been widely used to analyze and design microlenses of different conic sections on the tip of the SMF. It may be relevant to mention in this connection that the coupling optics involving hyperbolic microlens on the tip of the circular core step index single mode fiber (CCSISMF) in absence [4, 5] and presence [6] of possible misalignments as well as on the tip of circular core graded index single mode fiber (CCGISMF) [7] have been already reported based on previously formulated respective ABCD matrix [4, 5].

Moreover, the coupling optics involving hemispherical microlens on the tip of CCSISMF in absence [8] and presence [9] of possible misalignments as well as on the tip of CCGISMF [10] have also been already reported based on concerned theoretical ABCD matrix formalism [8]. The coupling optics involving parabolic microlens on the tip of CCSISMF [12] as well as on the tip of CCGISMF [13] has been recently reported based on prescribed relevant ABCD matrix formalism [11].

But the coupling efficiency of hemispherical microlens as well as parabolic microlens is impaired due to limited aperture while fabrication of hyperbolic microlens is limited by involved technique. Recently upside down tapered microlens (UDTML) on the fiber tip, designed by tapering the fiber end into a large hemispherical shape, has also emerged [15–17] side by side as a new novel lensing scheme in coupling optics. UDTML may be utilized to accumulate a huge amount of light from the LD [15]. A detailed work on formation and power distribution properties of UDTML has been already reported in Ref. [15] while the corresponding structure of the UDTML fiber end and the refractive index distribution has already been highlighted in Ref. [16]. Thus, the study of coupling optics involving UDTML on the tip of SMF is of huge importance. Based on the prescribed transformation ABCD matrix of UDTML [17], the studies of the coupling losses in case of LD to CCSISMF [18] as well as on CCGISMF [19] coupling via UDTML on the tip of such fibers have also been already reported. It may be relevant to mention in this connection that the Fresnel backward reflection has been neglected to investigate the coupling optics using UDTML on the tip of CCSISMF [18] and CCGISMF [19].

In this context it is worth mentioning that photonic crystal fibers (PCFs), also known as microstructured optical fibers, have attracted a considerable amount of attention recently, because of their unique properties that are not realized in conventional optical fibers (COFs). PCF is actually a unique type of pure silica optical fiber [20–22] with an array of air holes running along the entire length of the fiber,

reminiscent of a crystal lattice, which gives to this type of fiber, its name. The central air hole of the structure has been omitted to form the core (Figure 1). Based on the light-guiding mechanism, PCFs can be classified into two main categories. The first one, air-guided hollow core PCFs in which light is guided by the photonic band-gap (PBG) effect while the second one, index-guided solid core PCFs in which light is guided by the process of modified total internal reflection (MTIR). Because of high design flexibility of the PCFs compared to COFs, important optical properties can be tailored in PCFs [23, 24]. For index guiding solid core PCFs, these properties include endlessly single modeness, large mode area, high numerical aperture, high birefringence, high nonlinear coefficient, and tailorable large dispersion [23]. Moreover, PCFs can transport light with very low loss in certain wavelength where COFs possess very large loss [24]. Thus, in view of a wide range of favourable characteristics of PCFs, the study of this special kind of optical fiber is immensely necessitated.

Now, there are enormous amount of research works on microlenses like hyperbolic, hemispherical, parabolic, upside down tapered microlenses on the tip different types of circular core COFs which have enriched the literature [1–13, 15–19] in the context of coupling optics. However, as per as research and developments related with microlensing coupling schemes on the tip of circular core photonic crystal fibers (CCPCFs) are concerned, different research papers investigating coupling of LD to solid core PCF via hyperbolic [25, 26], hemispherical [27, 28], parabolic [29] microlenses in absence and presence of possible transverse and angular mismatches have been reported very recently using relevant ABCD matrix formalism. However, no such information is available regarding a study of coupling optics involving LD and CCPCF via UDTML on the tip of such fiber due to possible transverse and angular mismatches. Thus, our aim is to study the coupling losses due to possible transverse and angular misalignments in the case of a LD to CCPCF coupling via a UDTML on the tip of such fiber. Such investigation is important and pertinent for assessing the sensitivity of the

efficient coupler in the presence of these two kinds of misalignments.

In the first part of this paper, we theoretically investigate the coupling efficiencies between a semiconductor LD emitting light of wavelength $\lambda = 1.3 \mu\text{m}$ [3] and a series of typical CCPCFs with different air filling ratio d/Λ and lattice constant or hole pitch Λ [25–29] via UDTML of two different taper lengths [18] on the tip of these fibers in absence of possible transverse and angular misalignments. In the second part, we carry out the similar investigation for a LD emitting light of wavelength $\lambda = 1.5 \mu\text{m}$ [3]. A comparison between these two cases is performed. Finally, the transverse and angular misalignments are studied for CCPCFs having a specific air filling ratio d/Λ and lattice constant Λ excited with LD emitting light of a particular wavelength. As already stated, this analysis is based on previously derived simple ABCD matrix for refraction by a UDTML [17]. In fact, predictions of coupling optics by ABCD matrix method have produced excellent results as far as coupling of LD via UDTML of specific taper length on the tip of CCSISMF [18] and CCGISMF [19] are concerned. Concerned calculations need very little computations.

Further, we employ Gaussian field distributions for both the LD and the CCPCF. The present analysis, reported for the first time, contains significant new results in connection with the appropriate design of fiber geometry, i.e., core size, air hole pitch, the air hole size and the distribution of air holes, at a suitable wavelength emitted from the LD as well as that for the prediction of the suitable optogeometry of the UDTML. The results should be extremely important for the experimentalists, system designers and packagers who can, accordingly, mould and shape the desired UDTML at the CCPCF to achieve optimum coupling optics involving CCPCF in which air hole size, pitch, and distribution are additional degrees of freedom compared to COFs. Moreover, the results are extremely useful for assessing deeply the sensitivity of such coupler with reference to above types of mismatches.

ANALYSIS

Preview of UDTML Structure and Spot Sizes of CCPCF

In this analysis, we consider the structure of the UDTML fiber end drawn from a SMF of core radius ‘ a ’ as shown in Figure 1. Here, the radius of curvature R_0 and height ‘ h ’ of the spherical end are related to the radius of aperture ‘ d ’ by [16, 17]

$$R_0 = \frac{h^2 + d'^2}{2h} \quad (1)$$

where the radially symmetric axis OZ is actually the fiber axis and r and z represent the respective radial and axial coordinates, in the tapered region. The tapered surface equation is given by [16, 17]

$$r = d' \left(1 - \frac{z}{L} \right) \quad (2)$$

where L is the length of the cone including the tapered region.

Now, in our present study, we consider an all-silica CCPCF having a triangular lattice of uniform structure for the air-hole and glass matrix elongated along the total length of the propagation direction of the fiber, as shown in Figure 1. The air-holes, each of diameter d , are distributed symmetrically around a central silica defect, which is actually an omitted air-hole, acting as the core of the said CCPCF. The infinite air-hole matrix with lattice constant Λ and air filling ratio d/Λ has been considered to act as the cladding of the CCPCF. Since the effective cladding index n_{FSM} is lesser than that of the core-index n_{CO} , the fiber can guide light by PBG mechanism for shorter wavelengths and by the mechanism of MTIR as in case of a conventional step index fiber (CSF) for longer wavelengths [25–30].

Now, the fundamental modal field in a CCPCF is approximated as a Gaussian function [25–29, 31]

$$\psi_f = \exp \left[-\frac{x^2 + y^2}{w_{eff}^2} \right] \quad (3)$$

where w_{eff} corresponds to the spot size of the CCPCF.

The upper and lower limits of the propagation constants β of the guided modes through the core of the CCPCF satisfy [25–30, 32]

$$kn_{CO} > \beta > \beta_{FSM} \quad (4)$$

where, $k=2\pi/\lambda$ being the wave number associated with the operating wavelength λ , n_{CO} is the refractive index of silica as the core material and β_{FSM} is the propagation constant of the fundamental space-filling mode (FSM), which is the fundamental mode in the infinite photonic crystal cladding without any defect or core.

The effective cladding index or the index corresponding to the FSM is [25–30, 32]

$$n_{FSM} = \frac{\beta_{FSM}}{k} \quad (5)$$

The procedure for obtaining the value of n_{FSM} for the given parameters of the CCPCF at operating wavelength of light has been detailed once again in Appendix A for ready reference following [25–29]. Here all the coefficients are determined by applying the least square fitting method for the operating wavelengths $\lambda = 1.3\mu m$ and $\lambda = 1.5\mu m$, presented in Tables 1 and 2, respectively. These coefficients have been utilized for determining the values of n_{FSM} of the CCPCF for various values of lattice constant and the air filling ratio at any particular wavelength of interest [25–29].

The effective cladding index n_{FSM} can be utilized for finding the effective V -parameter of the CCPCF, treating the CCPCF like a CSF, with its cladding and core indices same as those of infinite photonic crystal structure and silica, respectively. Now the effective V value of the CCPCF is given by [25–30, 33]

$$V_{eff} = \frac{2\pi}{\lambda} a_{eff} \left[n_{CO}^2 - n_{FSM}^2 \right]^{1/2} \quad (6)$$

where, a_{eff} is the effective core radius which is assumed [25–30, 33, 34] to be $\Lambda/\sqrt{3}$ and λ is the operating wavelength.

Table 1: Values of All Coefficients Required for the Formulation of Effective Cladding

Index n_{FSM} at $\lambda = 1.3\mu m$.

$\lambda = 1.3\mu m$			
	$i = 0$	$i = 1$	$i = 2$
A_i	1.430434	0.003803	-0.000214
B_i	0.069387	-0.012541	0.000650
C_i	-0.375746	0.107635	-0.008799

Table 2: Values of All coefficients Required for the Formulation of Effective Cladding

Index n_{FSM} at $\lambda = 1.5\mu m$.

$\lambda = 1.5\mu m$			
	$i = 0$	$i = 1$	$i = 2$
A_i	1.432783	0.002170	-0.000036
B_i	0.063468	-0.007890	0.000147
C_i	-0.415418	0.114257	-0.009127

Then using Marcuse formula [31], the modal spot size w_{eff} , half of the mode field diameter (MFD) can be written as [25–30]

$$\frac{w_{eff}}{a_{eff}} = 0.65 + \frac{1.619}{V_{eff}^{3/2}} + \frac{2.879}{V_{eff}^6} \quad (7)$$

The spot size of the CCPCF, w_{eff} is obtained by using Eq. (7), where V_{eff} being the effective V -parameter, calculated from Eq. (6). The method of such calculation has been detailed in Appendix A following [25–30].

Formulation of microlens coupling scheme

The coupling scheme to be studied has been presented in Figure 1. Here, ‘ u ’ is the distance of separation between the LD and the UDTML end of the fiber. Again, in our analysis we use some usual approximations [2, 4–10, 12, 13, 18, 19, 25–29] like Gaussian field distributions for both the source and the fiber, perfect matching of the polarisation mode of the fiber field and that on the microlens surface, no transmission loss, sufficient angular width of the microlens to intercept the entire power radiated by the source for typical values of the microlens parameters employed. However, for the purpose of estimation of coupling optics using such LD and various kind of microlenses

[4–10, 12, 13, 18, 19, 25–29], we simply use Gaussian beam with the elliptical waist spot sizes since the LDs we usually employ have dimensions of the parallel and perpendicular junctions fairly comparable [18].

The field Ψ_u representing the output of the LD at a distance u from the UDTML surface is taken as [18, 19, 35]

$$\Psi_u = \exp\left[-\left(\frac{x^2}{w_{1x}^2} + \frac{y^2}{w_{1y}^2}\right)\right] \exp\left[-\frac{ik_1}{2} \cdot \frac{x^2 + y^2}{R_1}\right] \quad (8)$$

Here, w_{1x} and w_{1y} represent the spot sizes due to elliptical intensity profiles of the optical beams emitted from LD along two mutually perpendicular directions X and Y, one perpendicular and the other parallel to the junction planes, k_1 is the wave number in the incident medium and R_1 is the radius of curvature of the wavefronts from the LD. Our analysis is applicable to single frequency laser emitting only one spatial mode with a Gaussian intensity profile.

The UDTML transformed laser field Ψ_v on the fiber plane 2 (plane for which $z = z_L$) as indicated in Figure 1 can be expressed as [18,19, 35].

$$\Psi_v = \exp\left[-\left(\frac{x^2}{w_{2x}^2} + \frac{y^2}{w_{2y}^2}\right)\right] \exp\left[-\frac{ik_2}{2} \left(\frac{x^2}{R_{2x}} + \frac{y^2}{R_{2y}}\right)\right] \quad (9)$$

where, w_{2x} , w_{2y} are respectively microlens transformed spot sizes and R_{2x} , R_{2y} being the respective transformed radii of curvature of the refracted wavefronts in the X and Y directions and k_2 being the wave number in the microlens medium. The method of finding w_{2x} , w_{2y} , R_{2x} and R_{2y} in terms of w_{1x} , w_{1y} and R_1 with the relevant ABCD matrix for UDTML following [17–19] on the fiber tip is once again presented in the Appendix B for ready reference.

The source to fiber coupling efficiency via UDTML on the fiber tip is expressed in terms of well-known overlap integral as mentioned below [4–10, 12, 13, 18, 19, 25–29, 36]

$$\eta = \frac{\left| \iint \Psi_v \Psi_f^* dx dy \right|^2}{\iint |\Psi_v|^2 dx dy \iint |\Psi_f|^2 dx dy} \quad (10)$$

Therefore η_0 , the coupling efficiency in absence of misalignment, for CCPCF is given by [25–29].

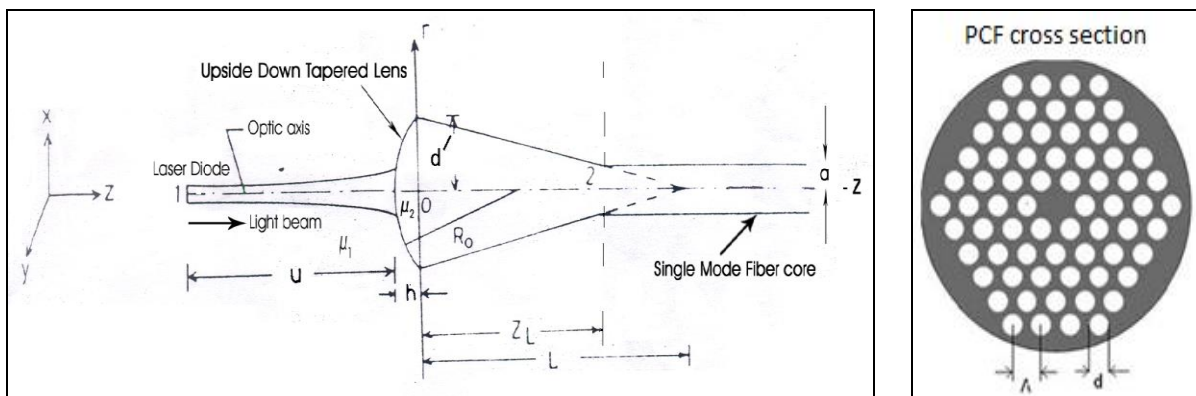


Fig. 1: Geometry of LD to CCPCF Coupling via UDTML on the Fiber Tip; μ_1 and μ_2 Stand for Refractive Indices of Incident and Microlens Media Respectively.

$$\eta_0 = \frac{4w_{2x}w_{2y}w_{eff}^2}{\left[\left(w_{eff}^2 + w_{2x}^2 \right)^2 + \frac{k_2^2 w_{2x}^4 w_{eff}^4}{4R_{2x}^2} \right]^{1/2} \left[\left(w_{2y}^2 + w_{eff}^2 \right)^2 + \frac{k_2^2 w_{2y}^4 w_{eff}^4}{4R_{2y}^2} \right]^{1/2}} \quad (11)$$

However, Eq. (11) can be obtained by employing Eqs. (3) and (9) in Eq. (10).

Misalignment considerations

An evaluation of the coupling efficiency in the presence of a transverse misalignment in the X-Y plane is based on the assumption that the center of the fiber is displaced to a point having coordinates (d_1, d_2) as shown in Figure 2.

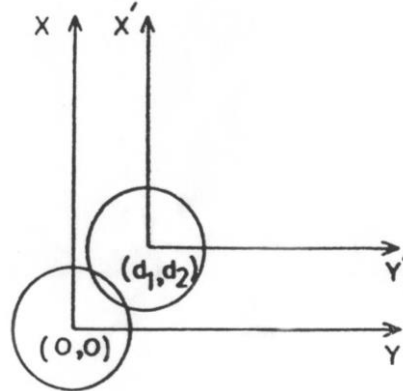


Fig. 2: Transverse Misalignment Between the Imaged Laser Spot and the Center of the Fiber.

From the well-known coordinate transformation technique, the relation between the primed and unprimed coordinates can be given by [14, 18, 26, 28, 29]

$$\begin{aligned} x &= x' + d_1 \\ y &= y' + d_2 \end{aligned} \quad (12)$$

In this case, the fundamental mode of the fiber can be represented as [14, 18, 26, 28, 29]

$$\psi_f = \exp \left[- \left(\frac{(x - d_1)^2}{w_{eff}^2} + \frac{(y - d_2)^2}{w_{eff}^2} \right) \right] \quad (13)$$

While the UDTML transformed laser field Ψv on the fiber plane 2 can be expressed as already mentioned by Eq. (9).

Employing Eqs. (9) and (13) in Eq. (10), one can obtain the coupling efficiency for only transverse offset as [14, 18, 26, 28, 29].

$$\eta_t = \eta_0 \exp \left[\frac{2d_1^2}{w_{eff}^2} \left\{ \frac{w_{2x}^2 (w_{2x}^2 + w_{eff}^2)}{(w_{eff}^2 + w_{2x}^2)^2 + \frac{k_2^2 w_{2x}^4 w_{eff}^4}{4R_{2x}^2}} - 1 \right\} \right] \exp \left[\frac{2d_2^2}{w_{eff}^2} \left\{ \frac{w_{2y}^2 (w_{2y}^2 + w_{eff}^2)}{(w_{eff}^2 + w_{2y}^2)^2 + \frac{k_2^2 w_{2y}^4 w_{eff}^4}{4R_{2y}^2}} - 1 \right\} \right] \quad (14)$$

where, η_0 , the coupling efficiency in absence of misalignment, is given by Eq. (11).

The angular misalignment of a small angle θ between the UDTML and the entrance of the fiber is shown in Figure 3.

In such a case the relation between primed and unprimed coordinates is given as [28, 29]

$$\begin{aligned} x &= x' \cos \theta + z' \sin \theta \\ y &= y' \\ z &= -x' \sin \theta + z' \cos \theta \end{aligned} \quad (15)$$

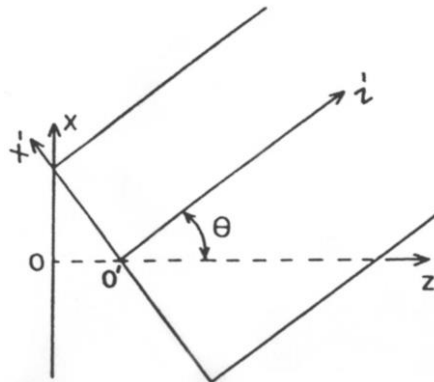


Fig. 3: Angular Mismatch Between the UDTML Transformed Input Face and the End Face of the Fiber.

We approximate Eq. (15) by using $\sin \theta = \theta$, $\cos \theta = 1$ [14] and $OO' = 0$ for small angular offset (Figure 3) and thus obtain

$$\begin{aligned} x &= x' + z' \theta \\ y &= y' \\ z &= -x' \theta + z' \end{aligned} \quad (16)$$

The UDTML transformed field on the fiber can be given by [14, 18, 26, 28, 29]

$$\Psi_v = \exp\left[-\left(\frac{x^2}{w_{2x}^2} + \frac{y^2}{w_{2y}^2}\right)\right] \exp\left[-\frac{ik_2}{2}\left(\frac{x^2}{R_{2x}} + \frac{y^2}{R_{2y}}\right)\right] \exp(-ik_2 z) \quad (17)$$

Using Eq. (16) and taking care of the fact that at the input end of the fiber z' is zero, one can readily express Eq. (17) in terms of primed coordinates as follows:

$$\Psi_v = \exp\left[-\left(\frac{x'^2}{w_{2x}^2} + \frac{y'^2}{w_{2y}^2}\right)\right] \exp\left[-\frac{ik_2}{2}\left(\frac{x'^2}{R_{2x}} + \frac{y'^2}{R_{2y}}\right)\right] \exp(ik_2 x' \theta) \quad (18)$$

Eqs. (3) and (18) are used in Eq. (10) to obtain the coupling efficiency η_a for a small angular mismatch θ in the case of circular core fiber as mentioned below [14, 18, 26, 28, 29].

$$\eta_a = \eta_0 \exp\left[-\frac{k_2^2 \theta^2}{2} \left\{ \frac{(w_{eff}^2 + w_{2x}^2) w_{2x}^2 w_{eff}^2}{(w_{eff}^2 + w_{2x}^2)^2} + \frac{k_2^2 w_{2x}^4 w_{eff}^4}{4R_{2x}^2} \right\}\right] \quad (19)$$

Eqs. (14) and (19) can be employed to predict coupling losses for transverse and angular mismatches, respectively.

The above formulations are used in next section to calculate coupling efficiencies in absence and presence of possible transverse and angular misalignments in case of coupling in between LD and a series of CCPCFs with different air filling ratio d/Λ and lattice constant Λ [25–29] via UDTML of different taper lengths [18] on the tip of these fibers.

RESULTS AND DISCUSSIONS

Optogeometrical Parameters under Consideration

Our formalism employs the relevant ABCD matrix under the paraxial approximation in order to predict the relevant coupling optics involving a LD and CCPCF via UDTML on the tip of the fiber. For the estimation of coupling efficiencies in absence and presence of any possible transverse and angular misalignments for a UDTML of specific taper length on the tip of CCPCF, we firstly use a

LD emitting light of wavelength $\lambda = 1.3\mu\text{m}$ with $w_{1x} = 1.081\mu\text{m}$, $w_{1y} = 1.161\mu\text{m}$ [3] and then LD emitting light of wavelength $\lambda = 1.5\mu\text{m}$ with $w_{1x} = 0.843\mu\text{m}$, $w_{1y} = 0.857\mu\text{m}$ [3]. The LD parameters used in this investigation are mentioned in Table 3. For the LD emitting light of abovementioned two respective wavelengths, we study the coupling efficiencies for a series of typical CCPCFs having different air filling ratio d/Λ and lattice constant Λ [25–29] as mentioned in Tables 4 and 5. Following [25–29], we choose three typical values of d/Λ , in the single moded region, ($d/\Lambda \leq 0.45$) corresponding to two arbitrary Λ value ($\Lambda = 4.5, 5.0\mu\text{m}$), as 0.35, 0.40, 0.45. Different calculated fiber spot sizes w_{eff} for these three d/Λ values corresponding to each Λ value ($\Lambda = 4.5, 5.0\mu\text{m}$) are then utilized [25–29] and shown in Tables 4 and 5 where we also present the relevant source positions with corresponding maximum coupling efficiencies for $\lambda = 1.3\mu\text{m}$ and $\lambda = 1.5\mu\text{m}$, respectively.

Table 3: Laser Diode Parameters

LD	Wavelength λ in μm	Spot size w_{1x} in μm	Spot size w_{1y} in μm	k_1 in μm^{-1}	k_2 in μm^{-1}
#1	1.3	1.081	1.161	0.4138	7.4915
#2	1.5	0.843	0.857	0.4775	6.4926

Again as earlier, following [4–10, 12, 13, 18, 19, 25–29], the maximum depth of the microlens h is taken as $6.0\mu\text{m}$ while the refractive index $\mu (= \mu_2/\mu_1)$ of the material of the microlens with respect to surrounding medium is once again taken as 1.55. The core and cladding refractive indices are chosen as 1.46 and 1.45, respectively. The core diameter is taken as $2a = 4.0\mu\text{m}$. An UDTML to be drawn from those typical fibers is chosen with $2d' = 6.0\mu\text{m}$ with UDTML length z_L as $23.3\mu\text{m}$ and $26.6\mu\text{m}$ corresponding to L being $70.0\mu\text{m}$ and $80.0\mu\text{m}$, respectively. The radius of curvature R_0 of the spherical end of the UDTML is taken as $90.0\mu\text{m}$ [18]. Further, as explained in earlier cases, since estimation of coupling efficiency on the basis of planar wave model differs insignificantly from that on the basis of spherical wave model [4–10, 12, 13, 18, 19, 25–29], we consider planar

wave model for the input beam from the laser facet for the sake of simplicity.

In our final part, for the computation of the coupling efficiencies in presence of possible transverse and angular mismatches, we use corresponding values of source positions for CCPCFs with air filling ratio d/Λ , lattice constant Λ having relevant spot sizes w_{eff} for excitation by LD #1, 2, respectively. The results corresponding to transverse and angular mismatches are reported in Tables 4 and 5. These investigations of coupling efficiencies are restricted around 0 to $2\mu\text{m}$ region for transverse offset and 0 to 2° region for angular offset [6, 7, 9, 18, 26, 28, 29]. This region is chosen so that the designers of microlenses can restrict the fabrication to such small mismatches.

Results for coupling scheme

From Tables 4 and 5, it is clear that the source position is a key parameter that affects directly the coupling efficiency or in other words the coupling efficiency can be improved through optimizing the working distance of the UDTML.

Now from the results obtained in Table 4, it is observed that for a taper length L of $70.0\mu\text{m}$, the maximum coupling efficiency can reach to 94.63 % when the source position $u = 4.7\mu\text{m}$ for the CCPCF with air filling ratio $d/\Lambda = 0.35$ and lattice constant $\Lambda = 5.0\mu\text{m}$ having spot size w_{eff} of $4.433909\mu\text{m}$, in case of excitation by a LD emitting light of above mentioned first wavelength. On the other hand, it is also observed that for a taper length L of $80.0\mu\text{m}$, the maximum coupling efficiency can reach to 97.29 % when the source position $u = 2.2\mu\text{m}$ for the same CCPCF with air filling ratio $d/\Lambda = 0.35$ and lattice constant $\Lambda = 5.0\mu\text{m}$ having spot size w_{eff} of $4.433909\mu\text{m}$, for excitation by a LD emitting light of the same wavelength.

In both of the Tables 4 and 5, it must be noted that the symbol η_{10}^* indicates coupling coefficient for transverse misalignment of $2\mu\text{m}$ along X direction only while η_{01}^* indicates coupling coefficient for transverse misalignment of $2\mu\text{m}$ along Y direction only. On the other hand, η_a^* represents coupling coefficient for angular mismatch of 2° .

Table 4: Results for optimum coupling efficiency for a series of CCPCFs with different air filling ratio d/Λ and lattice constant Λ via UDTML with different taper lengths L , at operating wavelength $\lambda = 1.3\mu\text{m}$.

$$d' = 3.0\mu\text{m}, a = 2.0\mu\text{m}, R_0 = 90.0\mu\text{m}, h = 6.0\mu\text{m}, \mu = 1.55$$

d/Λ	Λ (μm)	w_{eff} (μm)	$L = 70.0\mu\text{m}$					$L = 80.0\mu\text{m}$				
			u (μm)	η_0	η_{10}^*	η_{01}^*	η_a^*	u (μm)	η_0	η_{10}^*	η_{01}^*	η_a^*
0.35	4.5	3.957274	4.2	0.8933	0.7508	0.7399	0.6323	1.9	0.9291	0.7730	0.7608	0.6651
	5.0	4.433909	4.7	0.9463	0.8116	0.8013	0.6293	2.2	0.9729	0.8246	0.8135	0.6602
0.40	4.5	3.553313	3.5	0.8344	0.6828	0.6720	0.6246	1.4	0.8734	0.7107	0.6981	0.6567
	5.0	3.985642	4.2	0.8970	0.7545	0.7437	0.6329	1.9	0.9323	0.7765	0.7643	0.6654
0.45	4.5	3.236339	2.6	0.7812	0.6167	0.6066	0.6124	0.8	0.8183	0.6492	0.6367	0.6406
	5.0	3.627302	3.6	0.8460	0.6955	0.6848	0.6273	1.5	0.8848	0.7233	0.7107	0.6593

Table 5: Results for optimum coupling efficiency for a series of CCPCFs with different air filling ratio d/Λ and lattice constant Λ via UDTML with different taper lengths L , at operating wavelength $\lambda = 1.5\mu\text{m}$.

$$d' = 3.0\mu\text{m}, a = 2.0\mu\text{m}, R_0 = 90.0\mu\text{m}, h = 6.0\mu\text{m}, \mu = 1.55$$

d/Λ	Λ (μm)	w_{eff} (μm)	$L = 70.0\mu\text{m}$					$L = 80.0\mu\text{m}$				
			u (μm)	η_0	η_{10}^*	η_{01}^*	η_a^*	u (μm)	η_0	η_{10}^*	η_{01}^*	η_a^*
0.35	4.5	4.058139	3.9	0.6149	0.5504	0.5493	0.4439	1.7	0.6640	0.5943	0.5928	0.4797
	5.0	4.490145	4.4	0.6842	0.6212	0.6200	0.4630	2.1	0.7370	0.6669	0.6654	0.5010
0.40	4.5	3.625593	3.0	0.5437	0.4732	0.4722	0.4193	1.1	0.5855	0.5146	0.5133	0.4490
	5.0	4.026105	3.9	0.6096	0.5456	0.5444	0.4418	1.7	0.6584	0.5890	0.5875	0.4774
0.45	4.5	3.292278	2.0	0.4906	0.4112	0.4103	0.3971	0.4	0.5234	0.4494	0.4482	0.4199
	5.0	3.660019	3.1	0.5494	0.4798	0.4787	0.4213	1.2	0.5919	0.5217	0.5204	0.4515

Now, it is observed from Table 4 that the calculated no offset value of coupling loss for the most efficient fiber with air filling ratio $d/\Lambda = 0.35$, lattice constant $\Lambda = 5.0\mu\text{m}$ having respective spot size w_{eff} of $4.433909\mu\text{m}$ excited with LD #1 emitting light of wavelength $\lambda = 1.3\mu\text{m}$ is obtained as 0.2397 dB using UDTML with taper length $L=70.0\mu\text{m}$. Further, it is evident from the same Table that the calculated coupling loss for this fiber is 0.9066 dB for transverse misalignment of $2\mu\text{m}$ along X direction only while the calculated coupling loss for this specific fiber is 0.9620 dB for transverse misalignment of $2\mu\text{m}$ along Y direction only. It is also observed that the coupling loss for the said fiber is 2.0114 dB for angular mismatch of 2° . On the other hand, the calculated no offset value of coupling loss for the most efficient fiber with air filling ratio $d/\Lambda = 0.35$, lattice constant $\Lambda = 5.0\mu\text{m}$ having respective spot

size w_{eff} of $4.433909\mu\text{m}$ excited with LD #1 emitting light of wavelength $\lambda = 1.3\mu\text{m}$ is obtained as 0.1193 dB using UDTML with taper length $L=80.0\mu\text{m}$. Further, it is evident from the same Table that the calculated coupling loss for this fiber is 0.8376 dB for transverse misalignment of $2\mu\text{m}$ along X direction only while the calculated coupling loss for this specific fiber is 0.8964 dB for transverse misalignment of $2\mu\text{m}$ along Y direction only. It is also observed that the coupling loss for the said fiber is 1.8032 dB for angular mismatch of 2° .

Now, from Table 5, it is observed that in case of taper length L of $70.0\mu\text{m}$, the maximum coupling efficiency can reach to 68.42% when $u = 4.4\mu\text{m}$ for the CCPCF with $d/\Lambda = 0.35$ and $\Lambda = 5.0\mu\text{m}$ having spot size w_{eff} of $4.490145\mu\text{m}$, for excitation by a LD emitting light of abovementioned second wavelength.

However, for the taper length L of $80.0 \mu\text{m}$, the maximum coupling efficiency can reach to 73.70 % when $u = 2.1 \mu\text{m}$ for the same CCPCF with $d/\Lambda = 0.35$ and $\Lambda = 5.0 \mu\text{m}$ having spot size w_{eff} of $4.490145 \mu\text{m}$, for excitation by a LD emitting light of the same wavelength.

It is also observed from Table 5 that the calculated no offset value of coupling loss for the most efficient fiber with air filling ratio $d/\Lambda = 0.35$, lattice constant $\Lambda = 5.0 \mu\text{m}$ having respective spot size w_{eff} of $4.490145 \mu\text{m}$ excited with LD #2 emitting light of wavelength $\lambda = 1.5 \mu\text{m}$ is obtained as 1.6482 dB using UDTML with taper length $L=70.0 \mu\text{m}$. Further, it is evident from the same Table that the calculated coupling loss for this fiber is 2.0677 dB for transverse misalignment of $2 \mu\text{m}$ along X direction only while the calculated coupling loss for this specific fiber is 2.0761 dB for transverse misalignment of $2 \mu\text{m}$ along Y direction only. It is also found that the coupling loss for the said fiber is 3.3442 dB for angular mismatch of 2° . On the other hand, the calculated no offset value of coupling loss for the most efficient fiber with air filling ratio $d/\Lambda = 0.35$, lattice constant $\Lambda = 5.0 \mu\text{m}$ having respective spot size w_{eff} of $4.490145 \mu\text{m}$ excited with LD #2 emitting light of wavelength $\lambda = 1.5 \mu\text{m}$ is obtained as 1.3253 dB using UDTML with taper length $L=80.0 \mu\text{m}$. Further, it is evident from the same Table that the calculated coupling loss for this fiber is 1.7594 dB for transverse misalignment of $2 \mu\text{m}$ along X direction only while the calculated coupling loss for this specific fiber is 1.7692 dB for transverse misalignment of $2 \mu\text{m}$ along Y direction only. It is also observed that the coupling loss for the said fiber is 3.0016 dB for angular mismatch of 2° .

It is seen from these Tables that for excitation by LDs emitting light of wavelengths $\lambda = 1.3 \mu\text{m}$ and $\lambda = 1.5 \mu\text{m}$, respectively, the maximum coupling efficiency is achieved for the CCPCF with $d/\Lambda = 0.35$ and $\Lambda = 5.0 \mu\text{m}$ using a UDTML of taper length L

= $80.0 \mu\text{m}$ on its tip for excitation by LDs emitting light of the above mentioned two wavelengths. Moreover, the separation distances between the LD and the nearest point of the UDTML of a particular taper length have a very little difference comparatively in case of excitation by LDs emitting light of two wavelengths of practical interest. It is prominent that for a particular value of the lattice constant Λ , the coupling efficiency in absence as well as in presence of transverse misalignment decreases with increase in air filling ratio d/Λ for excitation by a LD emitting a particular wavelength of light. On the other hand, it is also observed that for a particular value of the air filling ratio d/Λ , the coupling efficiency in absence as well as in presence of transverse misalignment increases with increase in lattice constant Λ for excitation by a LD emitting a particular wavelength of light. However, the angular misalignment does not follow the similar pattern as that for transverse misalignment. Moreover, the comparison between these results of coupling efficiencies for the CCPCF with $d/\Lambda = 0.35$ and $\Lambda = 5.0 \mu\text{m}$ excited with two wavelengths predicts that the specific fiber with $d/\Lambda = 0.35$ and $\Lambda = 5.0 \mu\text{m}$ are most suitable in the context of the aforesaid coupling optics involving CCPCFs and this excitement is uniquely excellent for a LD emitting specially light of wavelength $\lambda = 1.3 \mu\text{m}$. Though the coupling efficiencies for CCPCF with $d/\Lambda = 0.35$ and $\Lambda = 5.0 \mu\text{m}$ excited with LD emitting light of wavelength $\lambda = 1.3 \mu\text{m}$ are 94.63% and 97.29% using UDTML with taper length $70.0 \mu\text{m}$ and $80.0 \mu\text{m}$ respectively, but the source position for the first case is $4.7 \mu\text{m}$ while that for the second case is $2.2 \mu\text{m}$ only. So far as the demand of achieving the merit of reasonable working distance to have maximum coupling efficiency on the tip of CCPCFs are concerned, this merit is acquired by CCPCF with $d/\Lambda = 0.35$ and $\Lambda = 5.0 \mu\text{m}$ using UDTML with taper length $70.0 \mu\text{m}$. However, the assembly of a LD in the close proximity of the UDTML within $4.7 \mu\text{m}$ is challenging to achieve in practice. But with the advent of new progress in nanotechnology, we are optimistic that the future technologist will involve any

breakthrough to realize our result and test it experimentally. Moreover, these values of V_{eff} for light of wavelengths $\lambda = 1.3\mu m$ and $\lambda = 1.5\mu m$, respectively, correspond to low V region which is very well known for evanescent wave coupling in optical fiber directional coupler.

Thus from Tables 4 and 5, it can be concluded that coupling efficiencies corresponding to transverse and angular misalignments show mutually complementary results. It is observed that the concerned coupling efficiency for transverse misalignment along X direction is always marginally higher than that for the transverse misalignment along Y direction. Moreover, with the increase of angular offset the coupling efficiency decreases relatively

faster than that for those obtained with increasing transverse offset as far as comparison of coupling efficiencies from no offset value is concerned. However, as the transverse mismatch is more sensitive than that of angular mismatch, the results for CCPCF with air filling ratio $d/\Lambda = 0.35$, lattice constant $\Lambda = 5.0\mu m$ and respective spot size w_{eff} of $4.433909\mu m$ are most suitable when excited with LD #1 emitting light of wavelength $\lambda = 1.3\mu m$. Consequently the coupling losses, both in absence and presence of possible misalignments, have been reduced for excitation by a LD emitting light of wavelength $\lambda = 1.3\mu m$ in comparison with that obtained for excitation by a LD emitting light of wavelength $\lambda = 1.5\mu m$.

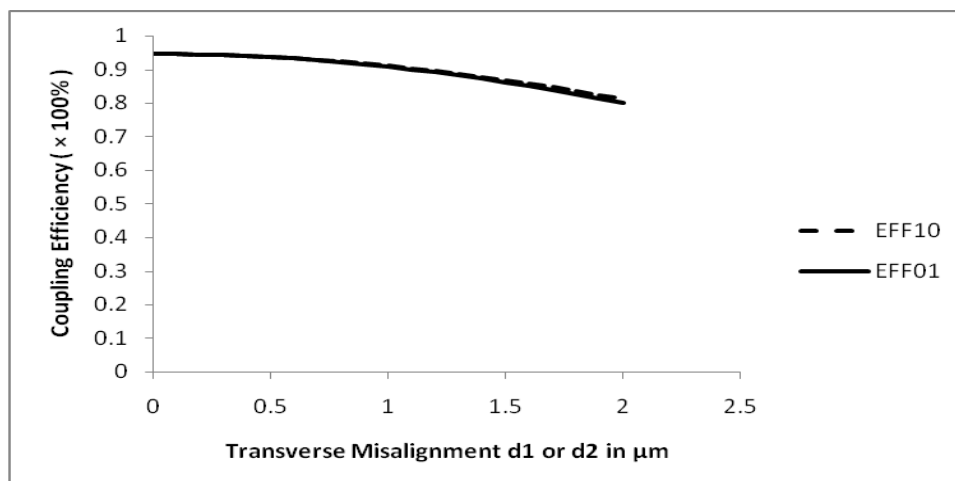


Fig. 4: Variation of Coupling Efficiency versus Transverse Misalignment for Most Suitable CCPCF Excited with LD #1 Emitting Light of Wavelength $\lambda = 1.3\mu m$.

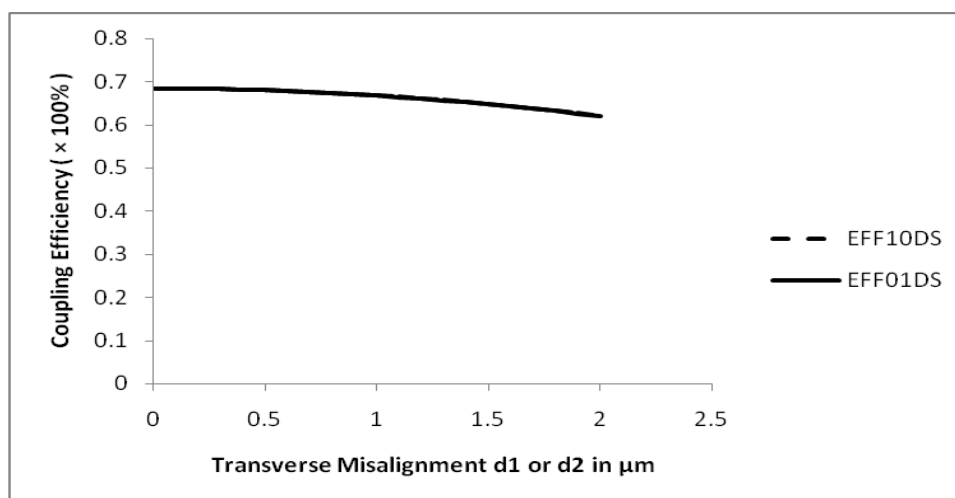


Fig. 5: Variation of Coupling Efficiency versus Transverse Misalignment for Most Suitable CCPCF Excited with LD #2 Emitting Light of Wavelength $\lambda = 1.5\mu m$.

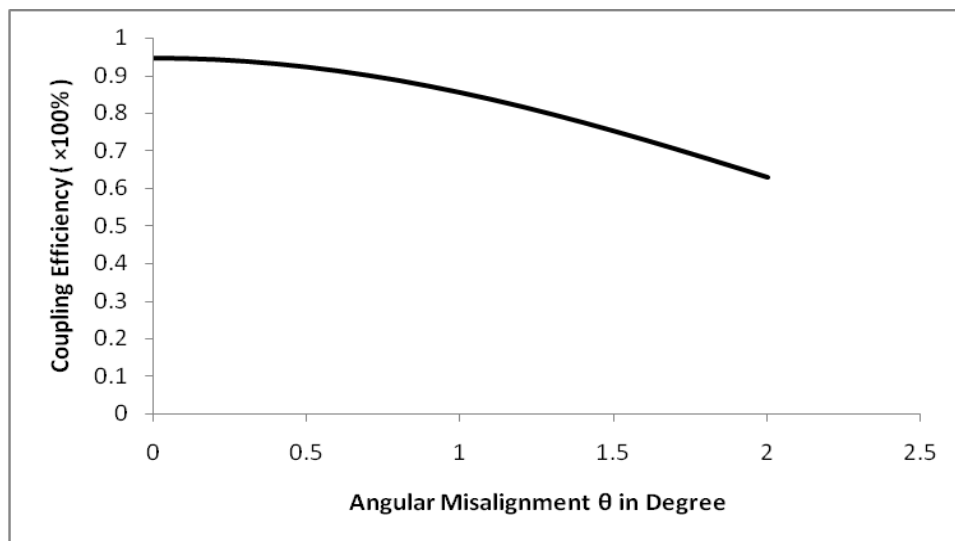


Fig. 6: Variation of Coupling Efficiency versus Angular Misalignment for Most Suitable CCPCF Excited with LD #1 Emitting Light of Wavelength $\lambda = 1.3 \mu\text{m}$.

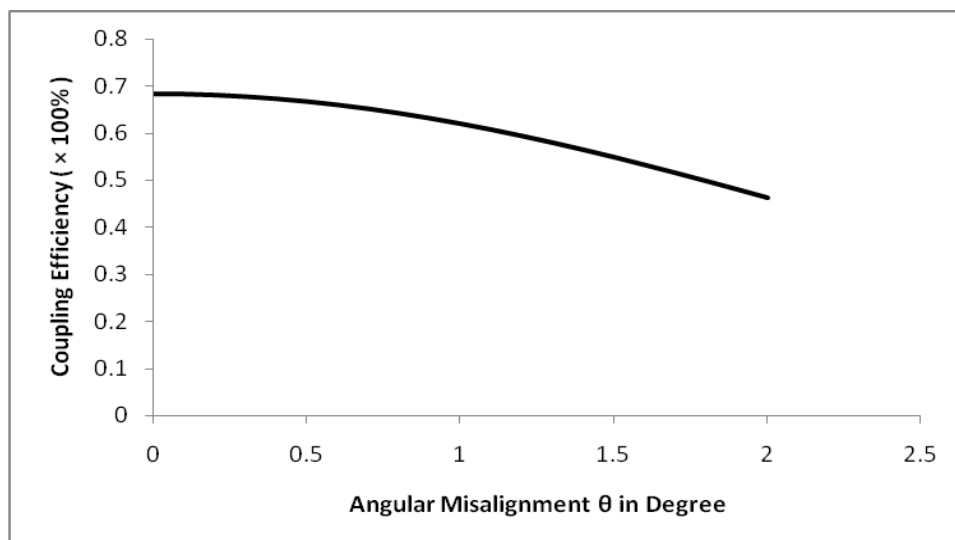


Fig. 7: Variation of Coupling Efficiency versus Angular Misalignment for Most Suitable CCPCF Excited with LD #2 Emitting Light of Wavelength $\lambda = 1.5 \mu\text{m}$.

For the typical estimation of knowledge of excitation by LDs emitting light of wavelengths $\lambda = 1.3 \mu\text{m}$ and $\lambda = 1.5 \mu\text{m}$, to the most suitable CCPCF with $d/\Lambda = 0.35$ and $\Lambda = 5.0 \mu\text{m}$ and respective w_{eff} of $4.433909 \mu\text{m}$ and $4.490145 \mu\text{m}$, via UDTML of taper length of $70.0 \mu\text{m}$ on its tip in presence of possible transverse misalignments, we present the variation of coupling efficiencies versus the transverse misalignments in Figures 4 and 5, respectively. In these Figures, the coupling efficiency designated as EFF10 is represented by the dashed line (corresponding to $d_2 = 0$ with d_1 varying from 0 to $2 \mu\text{m}$) while the

coupling efficiency EFF01 is represented by the solid line (corresponding to $d_1 = 0$ with d_2 varying from 0 to $2 \mu\text{m}$). In Figures 6 and 7, the curves present the variation of coupling efficiencies with the angular mismatch for the said fiber excited with LDs emitting light of wavelength $\lambda = 1.3 \mu\text{m}$ and $\lambda = 1.5 \mu\text{m}$, respectively.

CONCLUSIONS

We present, for the first time, to the best of our knowledge, a simple but realistic method for evaluation of coupling efficiency in between LD to a series of typical CCPCFs with different air filling ratio d/Λ and lattice

constant Λ via UDTML of two different taper lengths on its tip in absence and presence of possible transverse and angular mismatches by employing relevant ABCD matrix for refraction of UDTML. The best maximum coupling with optimization of appropriate source position is achieved for a CCPCF with air filling ratio of 0.35 and lattice constant of $5.0 \mu\text{m}$ when excited with LD emitting light of wavelength $\lambda = 1.3 \mu\text{m}$ using UDTML with taper length $L = 70 \mu\text{m}$. The optimized values of the taper length $L = 70.0 \mu\text{m}$ of the UDTML are playing a crucial role for excitement by light of both wavelengths of practical interest. In comparison with the other deeply involved rigorous methods like Finite Difference Method and Finite Element Method, the application of novel ABCD matrix has simplified the analysis as the concerned calculations need very little mathematical calculations. Moreover, the method predicts acceptable air filling ratio and lattice constant of the CCPCF from the point of view of fabrication of UDTML of allowable practical taper length. The technique developed should be useful in the system designing and packaging of suitable UDTML in coupling optics. Moreover, the results are also extremely useful for assessing deeply the sensitivity of the coupler with reference to two kinds of mismatches. However, the designers and packagers should be more careful in order to avoid angular mismatches as is visualized that a little angular misalignment causes a pronounced setback in comparison with little transverse misalignment.

APPENDIX A

The usual normalized parameters u and v for the infinite cladding region of the chosen CCPCF are given by [21, 25–30]

$$u = k\Lambda \left(n_{CO}^2 - \frac{\beta^2}{k^2} \right)^{1/2} \quad (\text{A1})$$

and

$$v = k\Lambda \left(n_{CO}^2 - 1 \right)^{1/2} \quad (\text{A2})$$

with

$$u^2 + w^2 = v^2 \quad (\text{A3})$$

In order to obtain the effective cladding index n_{FSM} , a basic air-hole at the centre of a

hexagonal unit cell is approximated to a circle in a regular photonic crystal [25–30, 32]. Then from relevant boundary conditions for the fields and their derivatives in terms of appropriate special functions, corresponding to a fixed value of v , obtained from Eq. (A2) for fixed Λ and λ -values, the concerned u values are computed for different d/Λ values at a particular λ from the following Eq., taking $n_{CO} = 1.45$ [21, 25–29]

$$wI_1(a_n w) [J_1(bu)Y_0(a_n u) - J_0(a_n u)Y_1(bu)] + uI_0(a_n w) [J_1(bu)Y_1(a_n u) - J_1(a_n u)Y_1(bu)] = 0 \quad (\text{A4})$$

$$\text{where, } a_n = \frac{d}{2\Lambda}, b = \left(\frac{\sqrt{3}}{2\pi} \right)^{1/2}$$

Using Eq. (A4), Russell has provided a polynomial fit to u , only for $d/\Lambda = 0.4$ and $n_{CO} = 1.444$. Further, for all d/Λ values of practical interest in the endlessly single mode region of a CCPCF, where d/Λ is less than 0.45, one should have a more general equation for wide applications [30].

The values of n_{FSM} are determined by replacing β/k in Eq. (A1) with n_{FSM} and this will lead to a modified simpler formulation of n_{FSM} as [25–30].

$$n_{FSM} = A + B \left(\frac{d}{\Lambda} \right) + C \left(\frac{d}{\Lambda} \right)^2 \quad (\text{A5})$$

where, A , B and C are the three different optimization parameters, dependent on both the relative hole-diameter or hole-size d/Λ and the lattice constant Λ .

Since optical communication window corresponds with two operating wavelengths of $1.3 \mu\text{m}$ and $1.5 \mu\text{m}$, this study finds the coefficients for these two wavelengths of practical interest for different possible hole-sizes and hole-pitches of the CCPCF. Such modification in such a fitting is advantageous in the sense that it will help for reducing the computation time since only nine coefficients are required in calculation instead of twenty seven coefficients [25–30].

Now, for each value of Λ with the variations of d/Λ , the n_{FSM} values corresponding to respective u values obtained from Eq. (A4) are determined. Applying least square fitting of n_{FSM} in terms of d/Λ to Eq. (A5) for a particular Λ , the values of A , B and C can be then estimated. The various values of A , B and C are then simulated for different Λ in the endlessly single mode region of the CCPCF, resulting in the empirical relations of A , B and C in Eq. (A5), in terms of Λ , as given in the following [25–30]

$$A = A_0 + A_1\Lambda + A_2\Lambda^2 \quad (A6)$$

$$B = B_0 + B_1\Lambda + B_2\Lambda^2 \quad (A7)$$

$$C = C_0 + C_1\Lambda + C_2\Lambda^2 \quad (A8)$$

where, A_i , B_i and C_i ($i=0,1$ and 2) are the optimization parameters for A , B and C , respectively. Computing A , B and C from Eqs. (A6-A8), one can find n_{FSM} directly for any d/Λ and Λ value at any particular λ using Eq. (A5) in the endlessly single mode region of the CCPCFs.

APPENDIX B

Considering the distance u of the LD from the UDTML end, q parameters of the Gaussian beams at the input laser facet and the output microlens fiber interface can be related by the ABCD matrix as follows:

The input and output parameters (q_1, q_2) of the light beam is related by [18, 19]

$$q_2 = \frac{Aq_1 + Au + B}{Cq_1 + Cu + D} \quad (B1)$$

where,

$$\frac{1}{q_{1,2}} = \frac{1}{R_{1,2}} - \frac{i\lambda_0}{\pi w_{1,2}^2 \mu_{1,2}} \quad (B2)$$

The ray matrix M for the UDTML on the fiber tip is given by [17–19]

$$M = \begin{pmatrix} A & B \\ C & D \end{pmatrix} \quad (B3)$$

where

$$A = r_2(z) - \frac{(1-\mu)r_1(z)}{\mu R_0} \quad (B4a)$$

$$B = \frac{r_1(z)}{\mu} \quad (B4b)$$

$$C = -\frac{(1-\mu)}{\mu R_0} \frac{dr_1(z)}{dz} + \frac{dr_2(z)}{dz} \quad (B4c)$$

$$D = \frac{1}{\mu} \frac{dr_1(z)}{dz} \quad (B4d)$$

The refractive index of the material of the microlens with respect to the incident medium is represented by $\mu (= \mu_2/\mu_1)$.

The z dependence of the above matrix elements can be explicitly expressed by substituting [17–19]

$$r_1(z) = -\frac{L}{\alpha} \left(1 - \frac{z}{L}\right)^{1/2} \sin k(z) \quad (B5a)$$

$$\frac{dr_1(z)}{dz} = \frac{1}{\left(1 - \frac{z}{L}\right)^{1/2}} \left\{ \cos k(z) + \frac{1}{2\alpha} \sin k(z) \right\} \quad (B5b)$$

$$r_2(z) = \left(1 - \frac{z}{L}\right)^{1/2} \left\{ \cos k(z) - \frac{1}{2\alpha} \sin k(z) \right\} \quad (B5c)$$

$$\frac{dr_2(z)}{dz} = \frac{A_0^2 L}{\left(1 - \frac{z}{L}\right)^{1/2} \alpha} \sin k(z) \quad (B5d)$$

where,

$$k(z) = \alpha \ln \left(1 - \frac{z}{L}\right) \quad (B6a)$$

$$\text{And } \alpha = \left(A_0^2 L^2 - 1/4\right)^{1/2} \quad (B6b)$$

L being the taper length or length of the cone including tapered region and A_0 is a constant given by

$$A_0 = \frac{1}{d'} \left(2 \ln \frac{n_{core}}{n_{clad}}\right)^{1/2} \quad (B7)$$

For a UDTML having aperture $2d'$

$$z_L = \frac{L(d' - a)}{d'} \quad (\text{B8})$$

In order to obtain w_{2x} , w_{2y} , the matrix is evaluated for $z = z_L$.

The transformed beam spot sizes and radii of curvature in the X and Y directions are found by using Eqs. (B4a-B4d) in Eqs. (B1) and (B2) and are given by

$$w_{2x,2y}^2 = \frac{A_1^2 w_{1x,1y}^2 + \frac{(\lambda_1^2 B_1^2)}{\pi^2 w_{1x,1y}^2}}{\mu(A_1 D_1 - B_1 C_1)} \quad (\text{B9})$$

$$\frac{1}{R_{2x,2y}} = \frac{A_1 C_1 w_{1x,1y}^2 + \frac{(\lambda_1^2 B_1 D_1)}{\pi^2 w_{1x,1y}^2}}{A_1^2 w_{1x,1y}^2 + \frac{(\lambda_1^2 B_1^2)}{\pi^2 w_{1x,1y}^2}} \quad (\text{B10})$$

where,

$$\lambda_1 = \frac{\lambda_0}{\mu_1} \quad (\text{B11})$$

$$A_1 = A + \frac{B_1}{R_1} \quad (\text{B12a})$$

$$B_1 = Au + B \quad (\text{B12b})$$

$$C_1 = C + \frac{D_1}{R_1} \quad (\text{B12c})$$

$$D_1 = Cu + D \quad (\text{B12d})$$

In plane wave front model, the radius of curvature R_1 of the wavefront from the laser facet $\rightarrow \infty$. This leads to $A_1=A$ and $C_1=C$.

REFERENCES

1. Presby HM, Edwards CA. Near 100% efficient fibre microlenses. *Electron. Lett.* 1992; 28: 582–584p.
2. Edwards CA, Presby HM, Dragone C. Ideal microlenses for laser to fiber coupling. *J. Lightwave Technol.* 1993; 11: 252–257p.
3. John J, Maclean TSM, Ghafouri-Shiraz H, et al. Matching of single-mode fibre to laser diode by microlenses at 1.5 μm wavelength. *IEE Proc. Optoelectron.* 1994; 141: 178–184p.
4. Gangopadhyay S, Sarkar SN. Laser diode to single-mode fibre excitation via hyperbolic lens on the fibre tip: Formulation of ABCD matrix and efficiency computation. *Opt. Commun.* 1996; 132: 55–60p.
5. Gangopadhyay S, Sarkar SN. ABCD matrix for reflection and refraction of Gaussian light beams at surfaces of hyperboloid of revolution and efficiency computation for laser diode to single-mode fiber coupling by way of a hyperbolic lens on the fiber tip. *Appl. Opt.* 1997; 36: 8582–8586p.
6. Gangopadhyay S, Sarkar SN. Misalignment considerations in laser diode to single-mode fibre excitation via hyperbolic lens on the fibre tip. *Opt. Commun.* 1998; 146: 104–108p.
7. Mukhopadhyay S, Sarkar SN. Coupling of a laser diode to single mode circular core graded index fiber via hyperbolic microlens on the fiber tip and identification of the suitable refractive index profile with consideration for possible misalignments. *Opt. Eng.* 2011; 50(4): 045004(1–9)p.
8. Gangopadhyay S, Sarkar SN. Laser diode to single-mode fiber excitation via hemispherical lens on the fiber tip: Efficiency computation by ABCD matrix with consideration for allowable aperture. *J. Opt. Commun.* 1998; 19: 42–44p.
9. Gangopadhyay S, Sarkar SN. Misalignment considerations in laser diode to single-mode fiber excitation via hemispherical lens on the fiber tip. *J. Opt. Commun.* 1998; 19: 217–221p.
10. Bose A, Gangopadhyay S, Saha SC. Laser diode to single mode circular core graded index fiber excitation via hemispherical microlens on the fiber tip: Identification of suitable refractive index profile for maximum efficiency with consideration for allowable aperture. *J. Opt. Commun.* 2012; 33(1): 15–19p.
11. Liu H, Liu L, Xu R, et al. ABCD matrix for reflection and refraction of Gaussian beams at the surface of a parabola of revolution. *Appl. Opt.* 2005; 44: 4809–4813p.
12. Liu H. The approximate ABCD matrix for a parabolic lens of revolution and its application in calculating the coupling efficiency. *Optik.* 2008; 119: 666–670p.

13. Mukhopadhyay S. Coupling of a laser diode to single mode circular core graded index fiber via parabolic microlens on the fiber tip and identification of the suitable refractive index profile with consideration for possible misalignments. *J. Opt.* 2016; 45(4): 312–323p.
14. Ghatak AK, Thyagarajan K. *Optical Electronics*. United Kingdom: Cambridge University Press; 1998, Chapters 10, 13, 15.
15. Yuan LB, Shou RL. Formation and Power Distribution Properties of an Upside Down taper Lens at the End of an Optical Fiber. *Sensors and Actuators*. 1990; A21-A23: 1158–1161p.
16. Yuan L, Qui A. Analysis of a single-mode fiber with taper lens end. *J. Opt. Soc. Am. A*. 1992; 9: 950–952p.
17. Mondal SK, Gangopadhyay S, Sarkar SN. Analysis of an upside-down taper lens end from a single-mode step index fiber. *Appl. Opt.* 1998; 37: 1006–1009p.
18. Mondal SK, Sarkar SN. Coupling of a laser diode to single-mode fiber with an upside-down tapered lens end. *Appl. Opt.* 1999; 38: 6272–6277p.
19. Mukhopadhyay S. Laser diode to circular core graded index single mode fiber excitation via upside down tapered microlens on the fiber tip and identification of the suitable refractive index profile. *J. Phys. Sci.* 2015; 20: 173–187p.
20. Russell PStJ. Photonic crystal fibers. *Science*. 2003; 299(5605): 358–362p.
21. Russell PStJ. Photonic-crystal fibers. *J. Lightwave Technol.* 2006; 24(12): 4729–4749p.
22. Bjarklev A, Broeng J, Bjarklev AS. *Photonic Crystal Fibres*. New York: Springer Science & Business Media Inc.; 2003.
23. Bhattacharya R, Konar S. Extremely large birefringence and shifting of zero dispersion wavelength of photonic crystal fibers. *Opt. & Laser Technol.* 2012; 44: 2210–2216p.
24. Sharma M, Borogohain N, Konar S. Index Guiding Photonic Crystal Fibers with Large Birefringence and Walk-Off. *J. Lightwave Technol.* 2013; 31: 3339–3344p.
25. Karak A, Kundu D, Mukhopadhyay S, et al. Investigation of coupling of a laser diode to photonic crystal fiber via hyperbolic microlens on the fiber tip by ABCD matrix formalism. *Opt. Eng.* 2015; 54(8): 086102(1–7)p.
26. Karak A, Kundu D, Sarkar SN. Optimum Launch Optics Involving Laser Excited Photonic Crystal Fibers via Hyperbolic Microlens on its Tip in Presence of Transverse and Angular Misalignments. *6th International Conference on Computers and Devices for Communication (CODEC)*; 2015 December 16–18; Institute of Radio Physics & Electronics, University of Calcutta, India: IEEE; 2015.
27. Chakraborty S, Roy D, Mukhopadhyay S, et al. An Investigative Study of Efficient Coupling Mechanism of a Hemispherical Microlens Tipped Single Mode Photonic Crystal Fiber to a Laser Diode by ABCD Matrix Formulation and Determination of the Optimal Separation Distance. *Optik*. 2017; 149: 81–89p.
28. Mukhopadhyay S. Misalignment studies in laser diode to hemispherical microlens tipped circular core photonic crystal fiber excitation. *J. for Foundations and Applications of Physics*. 2017; 4(2): 74–100p.
29. Mukhopadhyay S. Efficient Coupling of a Laser Diode to a Parabolic Microlens Tipped Circular Core Photonic Crystal Fiber using ABCD Matrix Formalism with Consideration for Possible Misalignments. *J. Opt.* 2018; 47(1): 47–60p.
30. Kundu D, Sarkar S. Prediction of propagation characteristics of photonic crystal fibers by a simpler, more complete and versatile formulation of their effective cladding indices. *Opt. Eng.* 2014; 53(5): 056111(1–6)p.
31. Marcuse D. Loss analysis of single-mode fiber splices. *J. Bell Syst. Tech.* 1977; 56(5): 703–718p.
32. Birks TA, Knight JC, Russell PStJ. Endlessly single-mode photonic crystal fiber. *Opt. Lett.* 1997; 22(13): 961–963p.
33. Koshiha M, Saitoh K. Applicability of classical optical fiber theories to holey fibers. *Opt. Lett.* 2004; 29(15): 1739–1741p.

34. Saitoh K, Koshiba M. Empirical relations for simple design of photonic crystal fibers. *Opt. Express*. 2005; 13(1): 267–274p.
35. Sarkar S, Thyagarajan K, Kumar A. Gaussian approximation of the fundamental mode in single-mode elliptic core fibers. *Opt. Commun*. 1984; 49: 178–183p.
36. Sarkar SN, Pal BP, Thyagarajan K. Lens coupling of laser diodes to monomode elliptic core fibers. *J. Opt. Commun*. 1986; 7: 92–96p.

Cite this Article

Sumanta Mukhopadhyay. Misalignment Studies in Laser Diode to Upside Down Tapered Microlens Tipped Circular Core Photonic Crystal Fiber Excitation. *Research & Reviews: Journal of Physics*. 2018; 7(3): 85–101p.